Predicting Error in Rigid-body, Point-based Registration

J. Michael Fitzpatrick[1]   Jay B. West[1]   Calvin R. Maurer, Jr. [2]

[1]Department of Computer Science, Vanderbilt University, Nashville, TN

[2]Departments of Neurosurgery and Biomedical Engineering, University of Rochester, Rochester, NY (Dr. Maurer was a research fellow in the Departments of Computer Science and Neurological Surgery, Vanderbilt University, Nashville, TN when this work was performed.)

Abstract

Guidance systems designed for neurosurgery, hip surgery, spine surgery, and for approaches to other anatomy that is relatively rigid can use rigid-body transformations to accomplish image registration. These systems often rely on point-based registration to determine the transformation, and many such systems use attached fiducial markers to establish accurate fiducial points for the registration, the points being established by some fiducial localization process. Accuracy is important to these systems, as is knowledge of the level of that accuracy. An advantage of marker-based systems, particularly those in which the markers are bone-implanted, is that registration error depends only on the fiducial localization error (FLE) and is thus to a large extent independent of the particular object being registered. Thus, it should be possible to predict the clinical accuracy of marker-based systems on the basis of experimental measurements made with phantoms or previous patients. This paper presents two new expressions for estimating registration accuracy of such systems and points out a danger in using a traditional measure of registration accuracy. The new expressions represent fundamental theoretical results with regard to the relationship between localization error and registration error in rigid-body, point-based registration.

Rigid-body, point-based registration is achieved by finding the rigid transformation that minimizes "fiducial registration error" (FRE), which is the root mean square distance between homologous fiducials after registration. Closed form solutions have been known since 1966. The expected value $\langle \mathrm{FRE}^2 \rangle$ depends on the number N of fiducials and expected squared value of FLE, $\langle \mathrm{FLE}^2 \rangle$, but in 1979 it was shown that $\langle \mathrm{FRE}^2 \rangle$ is approximately independent of the fiducial configuration $\mathcal{C}$. The importance of this surprising result seems not yet to have been appreciated by the registration community: Poor registrations caused by poor fiducial configurations may appear to be good due to a small FRE value.

A more critical and direct measure of registration error is the "target registration error" (TRE), which is the distance between homologous points other than the centroids of fiducials. Efforts to characterize its behavior have been made since 1989. Published numerical simulations have shown that $\langle \mathrm{TRE}^2 \rangle$ is roughly proportional to $\langle \mathrm{FLE}^2 \rangle / N$ and, unlike $\langle \mathrm{FRE}^2 \rangle$, does depend in some way on $\mathcal{C}$. Thus, FRE, which is often used as feedback to the surgeon using a point-based guidance system, is in fact an unreliable indicator of registration accuracy.

In this work we derive approximate expressions for $\langle \mathrm{TRE}^2 \rangle$, and for the expected squared alignment error of an individual fiducial. We validate both approximations through numerical simulations. The former expression can be used to provide reliable feedback to the surgeon during surgery and to guide the placement of markers before surgery, or at least to warn the surgeon of potentially dangerous fiducial placements; the latter expression leads to a surprising conclusion: Expected registration accuracy (TRE) is worst near the fiducials that are most closely aligned! This revelation should be of particular concern to surgeons who may at present be relying on fiducial alignment as an indicator of the accuracy of their point-based guidance systems.

Index Terms: Image registration, point-based, fiducial markers, accuracy prediction, target registration error.

I. Introduction

A common approach to surgical guidance is to perform point-based registration intraoperatively to tomographic images that were obtained preoperatively. Guidance is then provided by tracking a three-dimensional probe whose physical position is linked to the image position through the registration transformation. Systems have been developed for neurosurgery [1], [2], [3], [5], for hip surgery [6], and for radiotherapy [4], [7]. These systems take advantage of the approximate rigidity of the anatomy in the vicinity of the surgery, e.g., the contents of the head or the femur, so that the registration can be accomplished by a well-defined rigid-body transformation. The typical feedback provided by the registration system to the surgeon regarding the accuracy of the transformation

is confined to a measure of the degree of alignment of the points used in the registration. In this paper we argue that such measures are at best naive and at worst misleading, and we derive a new predictor of accuracy that is more reliable (a preliminary version of this work was presented at SPIE Medical Imaging 1998, in San Diego, CA, February 23, 1998 [8]). Our driving application lies in medical imaging, but our results should be of general interest to anyone engaged in point-based, rigid-body registration.

Image registration has been important for many years, but until CT made the three-dimensional cross-sectional image possible, the images to be registered were typically two dimensional. When the number K of physical dimensions is 3, as in the case of surgical guidance, the problem becomes considerably more difficult. The derivations that we present below are correct for arbitrary K. CT imaging became widely available (in the West) in the late 70's, and the field of three-dimensional image registration began to evolve rapidly in the early eighties [9]. A survey of medical image registration published in 1993 [10] listed 202 references; a new one to be published in early 1998 will list about 300 [11]. More than 70 of the publications in the latter survey are devoted to point-based registration; most of those involve rigid-body registration. In the typical medical application two volumetric images of a patient, such as X-ray Computed Tomography (CT) and Magnetic Resonance (MR) images, are to be registered with each other, as is done, for example, during preoperative planning, or one such image is to be registered directly to the patient, as is done at the beginning of intraoperative guidance. In either case registration errors can have serious consequences. Improved knowledge of their statistics will improve the quality of both surgical and diagnostic decisions.

Rigid-body registration is appropriate only when the imaged object is itself rigid, prominent examples being the human head, which for many diagnostic and therapeutic purposes may be considered to be rigid, the vertebrae, the pelvis, the femur, and other bones. The most accurate point-based methods utilize points defined by markers that are attached physically to bone through a skin incision [4], [6], [1], [5]. Because the positions of the points are trusted to determine the true transformation between spaces, they are termed "fiducial" points, and markers that are used to provide such points are called "fiducial markers" [12], [13], [14], [15], [16], [17], [1], [5], [18], [19], [20]. Point-based registration is achieved by finding the rigid transformation that brings the fiducial points in the two spaces into approximate alignment.

Error in the fiducial alignment, which can be directly measured by the registration system and provided as feedback to the surgeon, is the result of inevitable errors in the localization of the exact geometrical positions of these points. More importantly, these localization errors cause error in the registration of lesions, such as tumors, arteriovenous malformations, and the bones into which the markers are implanted, any of which may be the targets of surgery or diagnosis. Errors in the registration of these targets, which are the reason for the registration itself, cannot be measured by the registration system. Instead, the surgeon must rely on statistical predictors of these errors based on the known localization accuracy of the fiducials. Statistics on both fiducial registration error and target registration error have been studied for many years with target registration error being of most interest to the medical community. Target registration error can be expected to be related to the localization error of the fiducials, the fiducial configuration, and the position of the target itself, but heretofore no analytical expression for this relationship has been available. Lacking such an expression, researchers have resorted to numerical simulations to gain a qualitative notion of its form [21], [22], [1]. This simulation approach works to some extent, but it also has serious shortcomings. Its limitations spring from the time required to carry out a single simulation and the sparseness of the information contained in a set of simulations. What has been needed is an explicit expression. Such an expression reveals error patterns that are difficult to discern from simulations, they can be used in optimizations, and they put the field on a more solid footing. In this paper we provide such an expression. Specifically, we provide an approximate expression for the expected value of the squared target registration error. The expression is of particular value when fiducial markers are used. Unlike image registration procedures that use information contained in the object

being registered in order to find a matching transformation, the accuracy of fiducial-based registration is largely independent of the object to be registered. This independence arises because the accuracy of the registration is determined not by any characteristics of the object to be registered but by the number, placement, and localization accuracy of the fiducial markers. Once the localization accuracy has been measured for the given imaging modality via experiments with phantoms or with previous patients, it will be possible with the expression given here to determine the expected target registration accuracy for the current patient.

In addition to our expression for target registration error we present expressions for two different measures of fiducial registration error, one of which has been available, but unnoticed by the medical community, since 1979 [23]. By comparing these two expressions with our expression for target registration error, we show that as a predictor of registration accuracy fiducial registration error is not only unreliable but may in fact be misleading. This revelation should be of particular concern to surgeons who may at present be relying on fiducial alignment as an indicator of intraoperative registration accuracy for their patients.

II. THE POINT-BASED REGISTRATION PROBLEM

While there are variations on the size and shape of the landmarks or markers, their number and configuration, and the method for locating their positions, the basic mathematical statement of the point-based registration problem remains the same in most applications. In each case it is required to find a three dimensional translation $\mathbf{t}$ and rotation $\mathbf{R}$ that aligns one set of N points, $\mathbf{x}_i$, with a corresponding set, $\mathbf{y}_i$, $i = 1, 2, \ldots, N$, such that the distance d_i between corresponding points is minimized in the root-mean-square (RMS) sense. In medical applications each $\mathbf{x}_i$ represents the centroid of an anatomical landmark or one fiducial marker that has been localized in a three-dimensional, cross-sectional image of a patient (CT, for example). The point $\mathbf{y}_i$ is the corresponding centroid in a second image (MR, for example) or the centroid physically measured in the operating room, if the registration is being performed from image to patient (i.e., instead of from image to image) as part of a surgical guidance system. The RMS distance to be minimized is commonly termed the "fiducial registration error", or "FRE". Thus, the problem of registration reduces to finding a rotation and translation that minimizes FRE, where

$$\text{FRE}^2 \equiv \frac{1}{N} \sum_{i=1}^{N} |\mathbf{R}\mathbf{x}_i + \mathbf{t} - \mathbf{y}_i|^2. \tag{1}$$

If FRE = 0, the fiducial registration is perfect. Typically, however, because of errors in localizing the points, the fit will be only approximate. It may easily be shown [24] that the optimal translation is given by

$$\mathbf{t} = \overline{\mathbf{y}} - \mathbf{R}\overline{\mathbf{x}}, \tag{2}$$

where the bar indicates a mean over $i = 1, N$. The calculation of the optimal $\mathbf{R}$ is more difficult because of the nonlinear constraint that a rotation matrix be orthogonal. The first universal solution for $\mathbf{R}$ was published by Schönemann in 1966 [25] in a paper on the so-called "Orthogonal Procrustes Problem" in factor analysis[1]. Many others have produced independent solutions of the problem, either by methods equivalent to Schönemann's [27], [28] (see also [29]) or by representing rotations in terms of quaternions [30], [31], [32]. The problem is important to the statistical theory of shape [33], [34], [35] and to the fields of photogrammetry and robotics [36], [37], where it is known as the "Absolute Orientation Problem". In Schönemann's original work, which was unrelated to image

---

[1]The term "Procrustes" was originally pejorative. It was first used by Hurley and Cattell [26] in 1962 to express disapproval of a perceived tendency of some to distort one set of observations to support their claim that they fit another set. Hurley and Cattell were drawing an analogy to the way the character of the same name from Greek mythology stretched or squeezed visitors to fit his guest bed. The term is now common in the statistical theory of shape with no negative connotation attached.

registration, the goal was to find the $K \times K$ orthogonal matrix R that optimally transforms one set of $N \geq K$ observations X into another set of observations Y, where X and Y are observation matrices of dimension $N \times K$. Here "optimally" means that a quantity G is minimized, where

$$G \equiv \text{trace}(XR - Y)^t(XR - Y). \tag{3}$$

The image registration problem can be reduced to the Orthogonal Procrustes problem by letting row i of X be the elements of the demeaned vector $\hat{\mathbf{x}}_i = \mathbf{x}_i - \overline{\mathbf{x}}$ and row i of Y be $\hat{\mathbf{y}}_i = \mathbf{y}_i - \overline{\mathbf{y}}$, an approach first employed for a similar problem by Schönemann in 1970 [38]. With these assignments we have

$$\text{FRE}^2 = \frac{1}{N} \sum_{i=1}^{N} |\mathsf{R}\hat{\mathbf{x}}_i - \hat{\mathbf{y}}_i|^2 = G/N. \tag{4}$$

The solution that Schönemann found to minimize G (and FRE^2) is

$$R = BA^t, \tag{5}$$

where ADB^t is the singular value decomposition (SVD) of Y^tX. Thus,

$$Y^tX = ADB^t, \tag{6}$$

where A, D, and B are $K \times K$, A and B are orthogonal, D is diagonal, and the elements of D are non-negative. This solution, which we will call the "SVD" solution, was an improvement over a solution published in 1952 by Green [39] that was based on the concept of the square root of a symmetric matrix and required that X^tY be nonsingular, a restriction not required for the SVD solution.

III. Error Statistics

In the field of medical image registration the importance of the error statistics of point-based rigid-body registration was recognized by Evans as early as 1989 [40], [21] and has since been considered by many others [12], [41], [4], [22], [42], [43], [1]. Here the researchers in image registration were unaware of earlier, related work on the Procrustes problem. In 1979 [23] Sibson in a study of scaling theory first considered the effect of localization error on one of the point sets. He included translation in addition to rotation as part of the alignment procedure, as in the image registration problem. He observed that the distribution of the d_i was completely determined by localization error and not at all by any universal translation or rotation between the two point sets. Therefore he was able to confine his attention to the simple case in which the only difference between X and Y is caused by localization error. As a simplification he set the localization error to zero in the X space. Sibson incorporated a smallness parameter ϵ so that he could apply *perturbation theory* to find an approximate expression for FRE. Perturbation theory is a branch of mathematics which deals with the solution of problems that are by some measure close to a problem whose solution is known. By expressing the problem to be solved in terms of the known problem and a small positive parameter, ϵ, multiplied by a function representing the deviation from the soluble problem, it is possible to write the desired solution in terms of the known solution and a power series in ϵ. In Sibson's formalism

$$Y = X + \epsilon F, \tag{7}$$

where the elements of F are independent, identically distributed, random variables. Choosing a normal distribution, $\mathcal{N}(0, \sigma)$, he found that to second order G is chi-square distributed with $NK - \frac{1}{2}K(K+1)$ degrees of freedom. Thus its expected value is to second order:

$$\langle G \rangle = (NK - \tfrac{1}{2}K(K+1))\epsilon^2\sigma^2. \tag{8}$$

The next higher terms are $O(\epsilon^4)$, and Sibson reported that computer simulations showed excellent agreement with the $O(\epsilon^2)$ approximation. We can easily relate this result to the image registration literature by incorporating the definition of "fiducial localization error", or "FLE", which is the distance of the localized point from the (forever unknown) actual fiducial position before any alignment is done. We note that, because the K components of error are orthogonal and independent,

$$\langle \text{FLE}^2 \rangle = K\epsilon^2\sigma^2. \tag{9}$$

Using this relationship in Eq. 8 with $K = 3$ gives

$$\langle \text{FRE}^2 \rangle = (1 - 2/N)\langle \text{FLE}^2 \rangle. \tag{10}$$

Sibson's result has important implications: we see that FRE is independent of the fiducial configuration. In most medical applications, however, another error is of more concern: the "target registration error" at a spatial position **r**, denoted TRE(**r**), which is the distance between this point and the corresponding point in the other space after registration has been performed. The target may be any point in the space, and is commonly chosen within a point of interest, e.g. a lesion to be resected during surgery. We show in Section IV that TRE is strongly dependent on the fiducial configuration, thus leading to the conclusion that the traditional method of using FRE as a figure of merit for registration accuracy may in some cases lead to a bad choice of fiducial configuration, and to the surgeon having a false sense of security about the accuracy of the surgical guidance system. It has long been known that better point-based registrations, *i.e.*, smaller TREs, can be obtained by using more fiducial points to guide the registration [40], [21], [12], [41], [22]. More specifically, based on numerical simulations it has been conjectured that TRE has an approximate $N^{-1/2}$ dependence, given that points are added in some consistent way, such as choosing them randomly within or on the surface of a specified region, a sphere, for example, [21], [22], [1]. We have searched the Procrustes literature carefully but have found no work on this error statistic in that community. However, in 1991 Goodall did propose an expression for the first-order approximation of R based on Sibson's perturbation approach [34]. We begin the next section by deriving that expression.

IV. Derivation of the TRE statistic

Our goal is to find an approximate expression for $\langle \text{TRE}^2(\mathbf{r}) \rangle$. Following Sibson, we note that this statistic, like $\langle \text{FRE}^2 \rangle$, depends only on errors in localizing the fiducials, as opposed to gross motion between the two spaces. Also following Sibson, we will continue to treat the case in which the localization error is negligible in the "X" space. With these two assumptions we may use Eq. 7 above. The following expression results:

$$\begin{aligned} \langle \text{TRE}^2(\mathbf{r}) \rangle &= \langle |\mathbf{R}\mathbf{r} + \mathbf{t} - \mathbf{r}|^2 \rangle \\ &= \langle (rR + \epsilon t - r)(rR + \epsilon t - r)^t \rangle \\ &= \langle (r(R - I) + \epsilon t)(r(R - I) + \epsilon t)^t \rangle, \end{aligned} \tag{11}$$

where we have used matrix notation in the second and third lines, with r and t being row vectors. We have made explicit the fact that translation is first order in ϵ, as can be seen from Eqs. 2 and 7. Expanding the rotation matrix in ϵ, and noting that $R = I$ when $\epsilon = 0$, we have $R - I = \epsilon R^{(1)} + O(\epsilon^2)$. Thus, to second order

$$\langle \text{TRE}^2(\mathbf{r}) \rangle \approx \epsilon^2(\langle tt^t \rangle + 2\langle rR^{(1)}t^t \rangle + \langle rR^{(1)}R^{(1)t}r^t \rangle). \tag{12}$$

There are three terms on the right-hand side corresponding to pure translation, correlation between translation and rotation, and pure rotation. In this section we derive expressions for each of these

terms. We find that the second term is equal to zero, thus the rotational and translational motion are shown to be uncorrelated. The remainder of this section is divided into five parts—the derivation of an expression for $R^{(1)}$, the derivation of each of the three second-order terms in Eq. 12, and an examination of the resulting expression for $\langle \text{TRE}^2(\mathbf{r}) \rangle$.

A. $R^{(1)}$

We begin by imposing the orthogonality requirement on R:

$$
\begin{aligned}
R^t R = I &= (I + \epsilon R^{(1)t} + \text{O}(\epsilon^2))(I + \epsilon R^{(1)} + \text{O}(\epsilon^2)) \\
&= I + \epsilon(R^{(1)t} + R^{(1)}) + \text{O}(\epsilon^2).
\end{aligned}
$$

Therefore, $R^{(1)}$ is antisymmetric:

$$
R^{(1)t} = -R^{(1)}. \tag{13}
$$

We note from Eqs. 5 and 6 that for the optimal R, $Y^t X R = A D A^t$, from which we see that

$$
Y^t X R = R^t X^t Y. \tag{14}
$$

(Note that we will make no other use of the SVD solution. In fact in Schönemann's derivation this symmetry is established before decomposition is employed. Thus, we do not need to know the complete solution in order to derive the first order approximation.) For convenience we choose the origin of our coordinate system to lie at the centroid of the fiducial points, which means that

$$
\sum_{a=1}^{N} X_{ai} = 0 \tag{15}
$$

We use Eq. 7, for Y, but in order to account for translation, we must use demeaned versions of X and Y, as discussed before Eq. 4. We have demeaned X by our choice of origin; we demean Y by demeaning F,

$$
Y = X + \epsilon \hat{F}, \tag{16}
$$

where

$$
\hat{F}_{aj} = F_{aj} - \frac{1}{N} \sum_{b=1}^{N} F_{bj}. \tag{17}
$$

We now use Eq. 16, the expansion of R, and Eq. 13, in Eq. 14. The result is a series of equations for each power of ϵ. The linear terms yield this equation,

$$
X^t X R^{(1)} + R^{(1)} X^t X = X^t \hat{F} - \hat{F}^t X. \tag{18}
$$

We wish to solve this equation for $R^{(1)}$. The solution is made difficult by the fact that $R^{(1)}$ occurs multiplied on both the right and left. Following Goodall [34], we perform singular value decomposition on X to get $X = U \Lambda V^t$, where U and V are orthogonal and Λ is diagonal. Our assumption that the elements of F are identically distributed (see after Eq. 7) assures isotropy in the perturbations. Thus, we can without loss of generality orient our coordinate system in any direction we choose. We pick the orientation to be along the principal axes of the distribution of fiducial points, which means that $V = I$. Thus, we have

$$
X = U \Lambda. \tag{19}
$$

(Note: Neither this re-orientation nor the special positioning of the origin above is necessary to effect a solution to Eq. 18, nor for any part of the derivation that follows. However, they do reduce the complexity considerably, and they can be easily undone at the end.) Employing Eq. 19 enables us to solve Eq. 18,

$$
R_{ij}^{(1)} = \frac{\Lambda_{ii} Q_{ij} - \Lambda_{jj} Q_{ji}}{\Lambda_{ii}^2 + \Lambda_{jj}^2}, \tag{20}
$$

which is the result given by Goodall in 1991 [34], and similarly to Goodall we have defined

$$
Q = U^t \hat{F}. \tag{21}
$$

B. First term

From Eq. 15 we have that $\overline{\mathbf{x}} = 0$, which in Eq. 2 gives that $\mathbf{t} = \overline{\mathbf{y}}$, or

$$t_i = \frac{1}{N} \sum_{a=1}^{N} F_{ai}. \tag{22}$$

Thus, the first term in Eq. 12 becomes

$$\langle tt^t \rangle = \frac{1}{N^2} \sum_{i=1}^{K} \sum_{a=1}^{N} \sum_{b=1}^{N} \langle F_{ai} F_{bi} \rangle. \tag{23}$$

We assume that the elements of F are independent and identically distributed with variance σ^2. Thus, using δ_{ab} as the Kronecker delta function ($\delta_{\alpha\beta} = 0$ if $\alpha \neq \beta$; $\delta_{\alpha\alpha} = 1$),

$$
\begin{aligned}
\langle tt^t \rangle &= \frac{\sigma^2}{N^2} \sum_{i=1}^{K} \sum_{a=1}^{N} \sum_{b=1}^{N} \delta_{ab} \\
&= K\sigma^2/N.
\end{aligned}
$$

C. Second term

In terms of elements the second term of Eq. 12 has the form

$$\langle r R^{(1)} t^t \rangle = \langle \sum_{i=1}^{K} r_i \sum_{j \neq i}^{K} R_{ij}^{(1)} t_j \rangle, \tag{24}$$

where we have used the antisymmetry of $R^{(1)}$ to eliminate $i = j$ terms. Using Eqs. 20 and 22 gives

$$
\begin{aligned}
\langle r R^{(1)} t^t \rangle &= \frac{1}{N} \sum_{i=1}^{K} r_i \sum_{j \neq i}^{K} \langle \left(\frac{\Lambda_{ii} Q_{ij} - \Lambda_{jj} Q_{ji}}{\Lambda_{ii}^2 + \Lambda_{jj}^2} \right) \sum_{b=1}^{N} F_{bj} \rangle \\
&= \frac{1}{N} \sum_{i=1}^{K} r_i \sum_{j \neq i}^{K} \sum_{b=1}^{N} \left(\frac{\Lambda_{ii} \langle Q_{ij} F_{bj} \rangle - \Lambda_{jj} \langle Q_{ji} F_{bj} \rangle}{\Lambda_{ii}^2 + \Lambda_{jj}^2} \right)
\end{aligned}
$$

From Eqs. 21 and 17 we have that for $i \neq j$,

$$
\begin{aligned}
\langle Q_{ji} F_{bj} \rangle &= \sum_{a=1}^{N} (U_{aj} \langle F_{ai} F_{bj} \rangle - \frac{1}{N} \sum_{c=1}^{N} \langle F_{ai} F_{cj} \rangle) \\
&= 0, \tag{25}
\end{aligned}
$$

by our assumption of independence between distinct elements of F. Eqs. 21 and 17 also give us

$$
\begin{aligned}
\sum_{b=1}^{N} \Lambda_{ii} \langle Q_{ij} F_{bj} \rangle &= \sum_{a=1}^{N} U_{ai} \Lambda_{ii} \sum_{b=1}^{N} (\langle F_{aj} F_{bj} \rangle - \frac{1}{N} \sum_{c=1}^{N} \langle F_{cj} F_{bj} \rangle) \\
&= \sum_{a=1}^{N} U_{ai} \Lambda_{ii} \sum_{b=1}^{N} (\delta_{ab} - \frac{1}{N} \sum_{c=1}^{N} \delta_{bc}) \sigma^2 \\
&= 0,
\end{aligned}
$$

where we have used the independence of the elements of F in the second line to get the delta functions.

Thus, $\langle r R^{(1)} t^t \rangle$ is equal to zero.

D. Third term

In terms of elements the third term of Eq. 12 has the form

$$\langle rR^{(1)}R^{(1)t}r^t\rangle = \langle\sum_{i=1}^{K} r_i \sum_{j\neq i}^{K} R_{ij}^{(1)} \sum_{k\neq j}^{N} R_{kj}^{(1)} r_k\rangle, \tag{26}$$

where we have once again used the antisymmetry of $R^{(1)}$. Using Eq. 20 gives

$$\langle rR^{(1)}R^{(1)t}r^t\rangle = \sum_{i=1}^{K}\sum_{j\neq i}^{K}\sum_{k\neq j}^{K} \frac{\langle(\Lambda_{ii}Q_{ij} - \Lambda_{jj}Q_{ji})(\Lambda_{kk}Q_{kj} - \Lambda_{jj}Q_{jk})\rangle r_i r_k}{(\Lambda_{ii}^2 + \Lambda_{jj}^2)(\Lambda_{jj}^2 + \Lambda_{kk}^2)}. \tag{27}$$

We need to evaluate four terms involving expected values of products of Q's in the numerator. From Eq. 17 we have

$$\begin{aligned}\langle\hat{F}_{a\beta}\hat{F}_{b\delta}\rangle &= \langle(F_{a\beta} - \frac{1}{N}\sum_{c=1}^{N} F_{c\beta})(F_{b\delta} - \frac{1}{N}\sum_{d=1}^{N} F_{d\delta})\rangle \\ &= (\delta_{ab} - \frac{1}{N})\delta_{\beta\delta}\sigma^2. \end{aligned} \tag{28}$$

From Eq. 21 and Eq. 28 we have

$$\begin{aligned}\Lambda_{\alpha\alpha}\Lambda_{\gamma\gamma}\langle Q_{\alpha\beta}Q_{\gamma\delta}\rangle &= \sum_{a=1}^{N} U_{a\alpha}\Lambda_{\alpha\alpha}\sum_{b=1}^{N} U_{b\gamma}\Lambda_{\gamma\gamma}\langle\hat{F}_{a\beta}\hat{F}_{b\delta}\rangle \\ &= \delta_{\beta\delta}\sigma^2(\sum_{a=1}^{N} U_{a\alpha}U_{a\gamma}\Lambda_{\alpha\alpha}\Lambda_{\gamma\gamma} - \frac{1}{N}\sum_{a=1}^{N} U_{a\alpha}\Lambda_{\alpha\alpha}\sum_{b=1}^{N} U_{b\gamma}\Lambda_{\gamma\gamma}) \\ &= \delta_{\alpha\gamma}\delta_{\beta\delta}\Lambda_{\alpha\alpha}^2\sigma^2 \end{aligned} \tag{29}$$

where we have made use of the orthogonality of U, Eqs. 15 and 19, in the last line. Using Eq. 29 in Eq. 27 we get

$$\langle rR^{(1)}R^{(1)t}r^t\rangle = \sigma^2\sum_{i=1}^{K}\sum_{j\neq i}^{K} \frac{r_i^2}{\Lambda_{ii}^2 + \Lambda_{jj}^2}. \tag{30}$$

E. The resulting expression

Combining the three terms in Eq. 12 and using Eq. 9 we have finally that to second order

$$\langle\text{TRE}^2(\mathbf{r})\rangle \approx \langle\text{FLE}^2\rangle\left(\frac{1}{N} + \frac{1}{K}\sum_{i=1}^{K}\sum_{j\neq i}^{K}\frac{r_i^2}{\Lambda_{ii}^2 + \Lambda_{jj}^2}\right). \tag{31}$$

V. Fiducial misalignment and TRE

In Figure 1, we can see the simple geometric relationship between F_i, FRE and TRE. We start with the unperturbed fiducial position $\hat{x}_i$, perturb this by ϵF_i to give position y_i, and perform a registration which maps $\hat{x}_i$ to $\hat{x}_i R + \epsilon t$. Denoting the fiducial registration error measured at fiducial i as FRE_i, we can see that

$$\epsilon F_i = \text{TRE}(\hat{x}_i) - \text{FRE}_i. \tag{32}$$

We note that the expected squared value of ϵF_i is equal to $\langle\text{FLE}^2\rangle$. Squaring both sides of Eq. 32 and taking expected values gives that

$$\langle\text{FLE}^2\rangle = \langle\text{TRE}^2(\hat{x}_i)\rangle + \langle\text{FRE}_i^2\rangle - 2\langle\text{FRE}_i \cdot \text{TRE}(\hat{x}_i)\rangle. \tag{33}$$
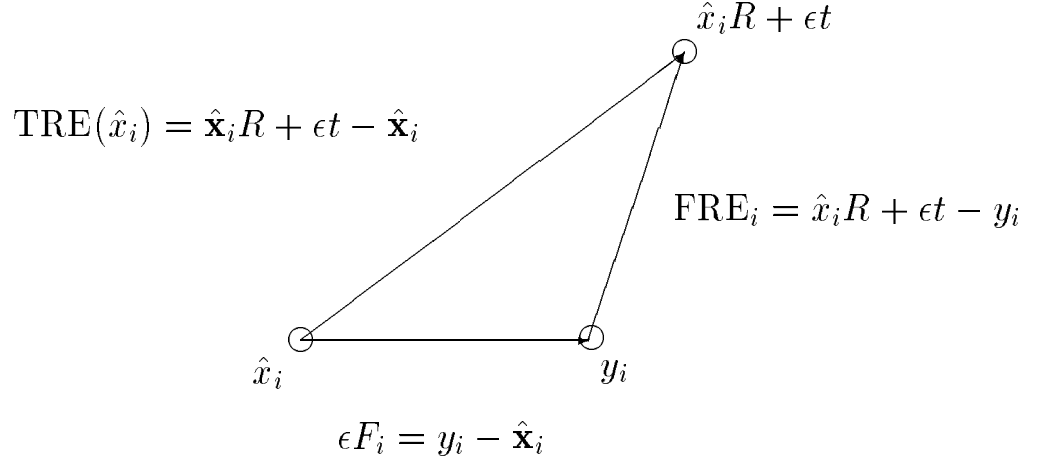
$$\mathrm{TRE}(\hat{x}_i) = \hat{\mathbf{x}}_i R + \epsilon t - \hat{\mathbf{x}}_i$$

$$\hat{x}_i R + \epsilon t$$

$$\mathrm{FRE}_i = \hat{x}_i R + \epsilon t - y_i$$

$$\hat{x}_i \qquad y_i$$

$$\epsilon F_i = y_i - \hat{\mathbf{x}}_i$$

Fig. 1. Geometrical relationship between ϵF_i, FRE, and TRE.

We will now show that the directions of FRE_i and $\mathrm{TRE}(\hat{x}_i)$ are uncorrelated, *i.e.*, that the third term is zero, yielding

$$\langle \mathrm{FLE}^2 \rangle = \langle \mathrm{TRE}^2(\hat{x}_i) \rangle + \langle \mathrm{FRE}_i^2 \rangle \tag{34}$$

Using Eq. 32, we may write

$$\langle \mathrm{FRE}_i \cdot \mathrm{TRE}(\hat{x}_i) \rangle = \langle \mathrm{TRE}^2(\hat{x}_i) \rangle - \epsilon \langle \mathrm{TRE}(\hat{x}_i) F_i^t \rangle.$$

Following Eq. 11, we rewrite $\mathrm{TRE}(\hat{x}_i)$ as $\hat{x}_i(R - I) + \epsilon t$, which to first order equals $\epsilon(\hat{x}_i R^{(1)} + t)$. First, we note that

$$\epsilon^2 \langle t F_i^t \rangle = \langle (\frac{1}{N} \sum_{j=1}^{N} F_j) F_i^t \rangle = \frac{\langle \mathrm{FLE}^2 \rangle}{N} \tag{35}$$

The remaining component of $\epsilon \langle \mathrm{TRE}(\hat{x}_i) F_i^t \rangle$ is $\epsilon^2 \langle \hat{x}_i R^{(1)} F_i^t \rangle$. Using the expression for $R_{ij}^{(1)}$ from Eq. 20 we have that

$$
\begin{aligned}
\hat{x}_i R^{(1)} F_i^t &= \sum_{j=1}^{K} \sum_{l \neq j}^{K} X_{ij} R_{jl}^{(1)} \hat{F}_{il} \\
&= \sum_{j=1}^{K} \sum_{l \neq j}^{K} X_{ij} F_{il} \left(\frac{\Lambda_{jj} Q_{jl} - \Lambda_{ll} Q_{lj}}{\Lambda_{jj}^2 + \Lambda_{ll}^2} \right).
\end{aligned} \tag{36}
$$

From Eq. 21 we recall the definition $Q = U^t \hat{F}$, thus allowing us to expand the Q terms in terms of U and $\hat{F}$. Performing this expansion, and taking expected values, we can see from Eq. 25 that $\langle F_{il} Q_{lj} \rangle = 0$ for $j \neq l$, hence the second term in the numerator has expected value zero. From this we may deduce that

$$
\begin{aligned}
\epsilon^2 \langle \hat{x}_i R^{(1)} \hat{F}_i^t \rangle &= \langle \sum_{j=1}^{K} \sum_{l \neq j}^{K} \sum_{m=1}^{N} \frac{X_{ij} \Lambda_{jj} U_{mj} F_{il} \hat{F}_{ml}}{\Lambda_{jj}^2 + \Lambda_{ll}^2} \rangle \\
&= \frac{\langle \mathrm{FLE}^2 \rangle}{K} \sum_{j=1}^{K} \sum_{l \neq j}^{K} \sum_{m=1}^{N} \frac{X_{ij} U_{mj} \Lambda_{jj} (\delta_{im} - \frac{1}{N})}{\Lambda_{jj}^2 + \Lambda_{ll}^2}.
\end{aligned} \tag{37}
$$

From Eqs. 15 and 19 we see that $\Lambda_{jj} \sum_{m=1}^{N} U_{mj}$ is zero, hence the $1/N$ component of the above sum goes to zero. We are left with only one term,

$$
\begin{aligned}
\frac{\langle \mathrm{FLE}^2 \rangle}{K} \sum_{j=1}^{K} \sum_{l \neq j}^{K} \sum_{m=1}^{N} \frac{X_{ij} U_{mj} \Lambda_{jj} \delta_{im}}{\Lambda_{jj}^2 + \Lambda_{ll}^2}
&= \frac{\langle \mathrm{FLE}^2 \rangle}{K} \sum_{j=1}^{K} \sum_{l \neq j}^{K} \frac{X_{ij} U_{ij} \Lambda_{jj}}{\Lambda_{jj}^2 + \Lambda_{ll}^2} \\
&= \frac{\langle \mathrm{FLE}^2 \rangle}{K} \sum_{j=1}^{K} \sum_{l \neq j}^{K} \frac{X_{ij}^2}{\Lambda_{jj}^2 + \Lambda_{ll}^2} \\
&= \mathrm{TRE}^2(\hat{x}_i) - \frac{\langle \mathrm{FLE}^2 \rangle}{N}.
\end{aligned}
\tag{38}
$$

Combining this result with that of Equation 35, and using this in Equation 35 gives that

$$
\langle \mathrm{FRE}_i \cdot \mathrm{TRE}(\hat{x}_i) \rangle = 0,
\tag{39}
$$

which verifies Eq. 34. We rearrange Eq. 34,

$$
\langle \mathrm{FRE}_i^2 \rangle = \langle \mathrm{FLE}^2 \rangle - \langle \mathrm{TRE}^2(\hat{x}_i) \rangle,
\tag{40}
$$

to emphasize the counter-intuitive result that small values of FRE_i are indicative of large values of $\mathrm{TRE}(\hat{x}_i)$. In order to check this expression, we may sum the expected values of FRE^2 over the N fiducials. This gives

$$
\sum_{i=1}^{N} \langle \mathrm{FRE}_i^2 \rangle = N \langle \mathrm{FLE}^2 \rangle - \sum_{i=1}^{N} \langle \mathrm{TRE}^2(\hat{x}_i) \rangle.
\tag{41}
$$

Using Eq. 31 for each value of $\langle \mathrm{TRE}^2(\hat{x}_i) \rangle$, we have that

$$
\sum_{i=1}^{N} \langle \mathrm{FRE}_i^2 \rangle = N \langle \mathrm{FLE}^2 \rangle - \langle \mathrm{FLE}^2 \rangle - \frac{\langle \mathrm{FLE}^2 \rangle}{K} \sum_{i=1}^{N} \sum_{j=1}^{K} \sum_{l \neq j}^{K} \frac{X_{ij}^2}{\Lambda_{jj}^2 + \Lambda_{ll}^2}.
\tag{42}
$$

Noting that $X^t X = \Lambda^t U^t U \Lambda = \Lambda^2$ by orthogonality of U, we may write

$$
\sum_{i=1}^{N} X_{ij}^2 = \sum_{i=1}^{N} X_{ji}^t X_{ij} = (X^t X)_{jj} = \Lambda_{jj}^2.
\tag{43}
$$

Thus we may make the simplification

$$
\begin{aligned}
\frac{\langle \mathrm{FLE}^2 \rangle}{K} \sum_{i=1}^{N} \sum_{j=1}^{K} \sum_{l \neq j}^{K} \frac{X_{ij}^2}{\Lambda_{jj}^2 + \Lambda_{ll}^2}
&= \frac{\langle \mathrm{FLE}^2 \rangle}{K} \sum_{j=1}^{K} \sum_{l \neq j}^{K} \frac{\Lambda_{jj}^2}{\Lambda_{jj}^2 + \Lambda_{ll}^2} \\
&= \frac{(K-1)\langle \mathrm{FLE}^2 \rangle}{2}.
\end{aligned}
\tag{44}
$$

This gives the result that

$$
\sum_{i=1}^{N} \langle \mathrm{FRE}_i^2 \rangle = (N - \tfrac{1}{2}(K+1)) \langle \mathrm{FLE}^2 \rangle.
\tag{45}
$$

which, substituting $K \epsilon^2 \sigma^2$ for $\langle \mathrm{FLE}^2 \rangle$, is exactly the result of Eq. 8 given by Sibson in 1979 [23].

VI. NUMERICAL SIMULATIONS

In order to verify the correctness of Eqs. 31 and 40, we performed some numerical simulations. First, we chose five values of N for which to perform the test: $N = 3, 4, 10, 20, 50$. For each of these values of N, we generated the correct number of fiducial positions randomly with uniform distribution within a cube of side 200 mm, and one target position randomly with uniform distribution within a cube of side 400 mm. In order to model fiducial localization error, we perturbed independently the x, y and z components of the fiducial positions in one space, using normally distributed independent random variables with zero mean and variance $1/3$ mm^2. In this way, we produced the same model as was used by Sibson in 1979 [23], and that is shown in Eq. 7. We registered the perturbed positions to the original ones, measuring the target registration error at the target position and at each fiducial position according to Eq. 11, and the fiducial registration error at each fiducial position according to Figure 1. One simulation consisted of 1,000,000 repetitions of the perturbation and registration step, allowing us to estimate the mean squared target and fiducial registration errors. Ten such simulations were performed, thus allowing us to estimate the standard deviation of the mean figures given in the previous step. In Table I we compare the simulated TRE results at the randomly chosen targets with those predicted by Eq. 31; in Table II we compare the simulated values of FRE_i^2 with those of $\mathrm{FLE}^2 - \mathrm{TRE}(\hat{\mathbf{x}}_i)^2$, where the fiducial index i is chosen so that the absolute percentage difference between the two quantities is maximized.

Number of fiducials	$\langle TRE^2 \rangle$ simulated (mean $\pm$ sd)	$\langle TRE^2 \rangle$ predicted	difference
3	4.7205 $\pm$ 0.0040	4.7186	-0.0019
4	2.1962 $\pm$ 0.0023	2.1962	0.0000
10	0.3441 $\pm$ 0.0004	0.3441	0.0000
20	0.1908 $\pm$ 0.0002	0.1907	-0.0001
50	0.0870 $\pm$ 0.0001	0.0870	0.0000

TABLE I

MEAN SQUARED TRE VALUES FROM SIMULATION VS. PREDICTED SQUARED TRE VALUE FROM EQ. 31 (ALL VALUES IN mm^2).

N	$\langle \mathrm{FRE}_i^2 \rangle$ simulated (mean $\pm$ sd)	$\langle \mathrm{FLE}^2 \rangle - \langle \mathrm{TRE}^2(\hat{\mathbf{x}}_i) \rangle$ simulated	difference
3	0.3150 $\pm$ 0.0002	0.3148 $\pm$ 0.0007	-0.0002
4	0.7301 $\pm$ 0.0005	0.7303 $\pm$ 0.0001	0.0002
10	0.8947 $\pm$ 0.0005	0.8943 $\pm$ 0.0001	-0.0004
20	0.9416 $\pm$ 0.0007	0.9407 $\pm$ 0.0001	-0.0009
50	0.9702 $\pm$ 0.0009	0.9695 $\pm$ 0.0000	-0.0007

TABLE II

SIMULATED MEAN SQUARED FRE VALUES VS. SIMULATED VALUES OF $\langle \mathrm{FLE}^2 \rangle - \langle \mathrm{TRE}^2 \rangle$ (ALL VALUES IN mm^2).

VII. DISCUSSION

Eq. 31 is the expression for the TRE statistic that we have sought. Like $\langle \mathrm{FRE}^2 \rangle$, it is proportional to $\langle \mathrm{FLE}^2 \rangle$, but, unlike $\langle \mathrm{FRE}^2 \rangle$, it also depends on the fiducial configuration. It is this dependence that makes it superior to $\langle \mathrm{FRE}^2 \rangle$ as a figure of merit for registration accuracy. For example, we find, not surprisingly, from this expression that for a given fiducial configuration the optimal position $\mathbf{r}$

for a target lies at the centroid of the configuration, which for our choice of origin means that $r_i = 0$. At that position the minimum expected squared error is achieved, which we find is $\langle \mathrm{FLE}^2 \rangle / N$. It can be seen from the derivation that $\langle \mathrm{FLE}^2 \rangle / N$ arises from the error in the centroid of the fiducials, the remainder being the result of rotational error in their configuration. It is thus clear from the derivation of this expression that a target at the centroid of the fiducial configuration is immune to rotational error in the transformation, which is represented in our derivations by R, and it is subject only to its translational error, which is represented by t. It can be seen also from the null value of the second term, derived in Section IV-C, that to second order the motion of the target due to rotation is uncorrelated with the motion due to translation. As the distance r of the target from the fiducial centroid increases, the error increases, approaching r^2 dependence. The error also increases as the configuration of the fiducials becomes smaller. In particular, suppose the shape of the configuration remains the same while its size is changed by some scale factor s. Thus, suppose X is multiplied by s. We note from Eq. 19 that $\Lambda^2 = X^t X$. Thus each element of Λ is scaled by s, and the summation in Eq. 31 is proportional to $1/s^2$. Thus, for large r/s, $\langle \mathrm{TRE}^2 \rangle$ increases as $(r/s)^2$.

Eq. 31 agrees with Hill's and Maurer's simulations [22], [1]. The simulations in Table I are the first ones to give a value of TRE^2 for a particular target and fiducial configuration, as opposed to merely a dependence of TRE^2 on, for example, the number N of fiducials or the value of the fiducial localization error. We note that in all cases the predicted results are within one standard deviation of those produced by the simulations. This leads us to believe that Eq. 31 is sufficiently accurate for surgical guidance, and that the terms of $O(\epsilon^4)$ and higher are approximately zero in expected value.

The expression in Eq. 31 also explains for the first time an $N^{-1/2}$ dependence for TRE reported by Evans [21] in 1993, by Hill in 1994 [22], and by Maurer in 1997 [1]. That dependence arises when restrictions imposed on choices of new points cause the denominator inside the summation to grow in proportion to N. While that dependence can be established for any value of K, we will specialize to the image registration problem now by setting $K = 3$. Since the origin is at the centroid of X, it is easy to show that if $i, j, k =$ permutation of $1, 2, 3$, then $\Lambda_{ii}^2 + \Lambda_{jj}^2$ is the moment of inertia M_k of the fiducial configuration about principal axis k. We note that $M_k = N \times f_k^2$, where f_k is the RMS distance of the fiducials from principal axis k. With this substitution we find that

$$\langle \mathrm{TRE}^2(\mathbf{r}) \rangle \approx \frac{\langle \mathrm{FLE}^2 \rangle}{N} \left(1 + \frac{1}{3} \sum_{k=1}^{3} \frac{d_k^2}{f_k^2} \right). \tag{46}$$

where d_k is the distance of the target from principal axis k. Thus, when N is increased by adding additional fiducial points, the expected $N^{-1/2}$ dependence occurs when points are added such that their RMS distance to the three axes remains constant.

Eq. 46, like Eq. 40, can be divided into translational error, FLE^2/N, and rotational error, the three components of which are inversely proportional to the spread of the fiducials about the corresponding axis. From Eq. 46 it may be deduced that a fiducial configuration that lies close to one of its own principal axes, *i.e.*, one which is almost collinear, will give rise to large TRE values at locations distant from the line of fiducials. It is also easy to see from Eq. 46 that isocontours of $\langle \mathrm{TRE}^2 \rangle$ are ellipsoidal and are centered at the centroid of the fiducial configuration. This finding explains the ellipsoidal isocontours of TRE^2 observed recently by Maurer [1] and by Darabi [44].

In some cases it may be known that the motion is entirely two-dimensional. In that case the term in parentheses in Eq. 31 reduces to $1 + d^2/(2f^2)$, where d is the distance of the target from the origin and f is the RMS distance of the fiducials from the origin.

From Eq. 40, we can see that TRE is expected to be worst at the places where FRE is best, i.e. near pairs of fiducial points that are in close alignment. From Table II, we can see that the results of the simulations are in excellent agreement with those predicted by Eq. 40. In fact, the agreement is

so close (in all cases the predicted values are within two standard deviations of the simulated values, despite the fact that the fiducial giving the worst agreement was chosen) that we are led to the same statement for Eq. 40 as was made for Eq. 31, *i.e.*, that the expression is sufficiently accurate for use in surgical guidance. The intuitive explanation for the relationship described by Eq. 40 is that the largest motion occurs at those fiducials that lie farthest away from the centroid: A small change in the rotation parameter will have little effect on the positions of the fiducials that are close to the centroid, but the relatively large motion at a point distant from the centroid may be used to bring a distant fiducial pair into close correspondence, thus reducing FRE_i. However, while the overall quality of the registration is expected to be improved by this change in R due to a single fiducial pair, the error due to the rotational misregistration becomes large as the distance from the fiducial centroid increases. In any case, both Eqs. 40 and 31 should serve as a stern warning to those who would use fiducial registration error as a measure of the quality of point-based registration.

VIII. Conclusion

With Eq. 31 we have provided an approximate answer to a long-standing question in point-based, rigid-body image registration: How does target registration error depend on the relative positions of the target and the fiducial points? Our approximation agrees closely with simulations, both those reported here and those reported by others in previous publications, showing that it is an excellent indicator of target registration error. Eq. 10 shows that overall fiducial alignment is by comparison a poor indicator of target registration accuracy, and Eq. 40 shows that individual fiducial alignment is worse. These two equations, although derived using approximations, are in extremely close agreement with simulations.

The availability of Eq. 31 puts the theory of image registration on a more solid footing. It also has immediate practical application for surgical guidance systems that rely on fiducial markers. It can provide the surgeon with more meaningful feedback regarding the accuracy of guidance during surgery, and it can guide the surgeon in placing the fiducials before surgery. Eqs. 10 and 40, on the other hand, serve as a warning that fiducial alignment alone should not be trusted as an indicator of registration success.

IX. Acknowledgement

References

[1] C. R. Maurer, Jr., J. M. Fitzpatrick, M. Y. Wang, R. L. Galloway, Jr., R. J. Maciunas, and G. S. Allen, "Registration of head volume images using implantable fiducial markers", *IEEE Trans. Med. Imaging*, vol. 16, pp. 447–462, 1997.

[2] K. Darabi, P. Grunert, and A. Perneczky, "Accuracy of intraoperative navigation using skin markers", in *Computer Assisted Radiology and Surgery 1997*, H. U. Lemke, M. W. Vannier, and K. Inamura, Eds., pp. 920–924. Springer-Verlag, Berlin, 1997.

[3] J. G. Golfinos, B. C. Fitzpatrick, L. R. Smith, and R. F. Spetzler, "Clinical use of a frameless stereotactic arm: Results of 325 cases", *J. Neurosurg.*, vol. 83, pp. 197–205, 1995.

[4] D. Jones, D. A. Christopherson, J. T. Washington, M. D. Hafermann, J. W. Rieke, J. J. Travaglini, and S. S. Vermeulen, "A frameless method for stereotactic radiotherapy", *Br. J. Radiol.*, vol. 66, pp. 1142–1150, 1993.

[5] F. C. Vinas, L. Zamorano, R. Buciuc, Q. H. Li, F. Shamsa, Z. Jiang, and F. G. Diaz, "Application accuracy study of a semipermanent fiducial system for frameless stereotaxis", *Comput. Aided Surg.*, vol. 2, pp. 257–263, 1997.

[6] R. H. Taylor, B. D. Mittelstadt, H. A. Paul, W. Hanson, P. Kazanzides, J. F. Zuhars, B. Williamson, B. L. Musits, E. Glassman, and W. L. Bargar, "An image-directed robotic system for precise orthopaedic surgery", *IEEE Trans. Robotics Automat.*, vol. 10, pp. 261–275, 1994.

[7] F. J. Bova, J. M. Buatti, W. A. Friedman, W. M. Mendenhall, C. C. Yang, and C Liu, "The University of Florida frameless high-precision stereotactic radiotherapy system", *Int. J. Radiation Oncology Biol. Phys.*, vol. 38, pp. 875–882, 1997.

[8] J. M. Fitzpatrick, J. West, and C. R. Maurer, Jr., "Derivation of expected registration error for rigid-body, point-based image registration", *Medical Imaging 1998: Image Processing*, 1998 (To appear).

[9] G. Q. Maguire, Jr., M. E. Noz, E. M. Lee, and J. H. Schimpf, "Correlation methods for tomographic images using two and three dimensional techniques", in *Information Processing in Medical Imaging 1985*, S. L. Bacharach, Ed., pp. 266–279. Martinus Nijhoff Publishers, Dordrecht, 1986.

[10] C. R. Maurer, Jr. and J. M. Fitzpatrick, "A review of medical image registration", in *Interactive Image-Guided Neurosurgery*, R. J. Maciunas, Ed., pp. 17–44. American Association of Neurological Surgeons, Park Ridge, IL, 1993.

[11] J. B. A. Maintz and M. A. Viergever, "A survey of medical image registration", *Med. Image Anal.*, vol. 2, 1998 (To appear).

[12] V. R. Mandava, J. M. Fitzpatrick, C. R. Maurer, Jr., R. J. Maciunas, and G. S. Allen, "Registration of multimodal volume head images via attached markers", *Medical Imaging VI: Image Processing*, vol. Proc. SPIE 1652, pp. 271–282, 1992.

[13] C. R. Maurer, Jr., J. M. Fitzpatrick, M. Y. Wang, and R. J. Maciunas, "Estimation of localization accuracy for markers in multimodal volume images", *Proc. Annu. Int. Conf. IEEE Eng. Med. Biol. Soc.*, vol. 15, pp. 124–125, 1993.

[14] C. R. Maurer, Jr., G. B. Aboutanos, B. M. Dawant, S. Gadamsetty, R. A. Margolin, R. J. Maciunas, and J. M. Fitzpatrick, "Effect of geometrical distortion correction in MR on image registration accuracy", *Medical Imaging 1994: Image Processing*, vol. Proc. SPIE 2167, pp. 200–213, 1994.

[15] C. R. Maurer, Jr., G. B. Aboutanos, B. M. Dawant, R. A. Margolin, R. J. Maciunas, and J. M. Fitzpatrick, "Registration of CT and MR brain images using a combination of points and surfaces", *Medical Imaging 1995: Image Processing*, vol. Proc. SPIE 2434, pp. 109–123, 1995.

[16] C. R. Maurer, Jr., G. B. Aboutanos, B. M. Dawant, S. Gadamsetty, R. A. Margolin, R. J. Maciunas, and J. M. Fitzpatrick, "Effect of geometrical distortion correction in MR on image registration accuracy", *J. Comput. Assist. Tomogr.*, vol. 20, pp. 666–679, 1996.

[17] M. Y. Wang, C. R. Maurer, Jr., J. M. Fitzpatrick, and R. J. Maciunas, "An automatic technique for finding and localizing externally attached markers in CT and MR volume images of the head", *IEEE Trans. Biomed. Eng.*, vol. 43, pp. 627–637, 1996.

[18] J. Rousseau, P. Clarysse, S. Blond, D. Gibon, C. Vasseur, and X. Marchandise, "Validation of a new method for stereotactic localization using MR imaging", *J. Comput. Assist. Tomogr.*, vol. 15, pp. 291–296, 1991.

[19] J. Rousseau, D. Gibon, P. Clarysse, J. P. Pruvo, S. Blond, and X. Marchandise, "Une méthode de repérage stéréotaxique par IRM", *J. Med. Nucl. Biophys.*, vol. 16, pp. 374–379, 1992.

[20] P. Clarysse, D. Gibon, J. Rousseau, S. Blond, C. Vasseur, and X. Marchandise, "A computer-assisted system for 3-D frameless localization in stereotaxic MRI", *IEEE Trans. Med. Imaging*, vol. 10, pp. 523–529, 1991.

[21] A. C. Evans, T. M. Peters, D. L. Collins, P. Neelin, and C. Gabe, "Image registration based on discrete anatomic structures", in *Interactive Image-Guided Neurosurgery*, R. J. Maciunas, Ed., pp. 63–80. American Association of Neurological Surgeons, Park Ridge, IL, 1993.

[22] D. L. G. Hill, D. J. Hawkes, M. J. Gleeson, T. C. S. Cox, A. J. Strong, W.-L. Wong, C. F. Ruff, N. Kitchen, D. G. T. Thomas, J. E. Crossman, C. Studholme, A. J. Gandhe, S. E. M. Green, and G. P. Robinson, "Accurate framless registration of MR and CT images of the head: Applications in surgery and radiotherapy planning", *Radiology*, vol. 191, pp. 447–454, 1994.

[23] R. Sibson, "Studies in the robustness of multidimensional scaling: Perturbational analysis of classical scaling", *J. R. Statist. Soc. B*, vol. 41, pp. 217–229, 1979.

[24] C. R. Maurer, Jr., G. B. Aboutanos, B. M. Dawant, R. J. Maciunas, and J. M. Fitzpatrick, "Registration of 3-D images using weighted geometrical features", *IEEE Trans. Med. Imaging*, vol. 15, pp. 836–849, 1996.

[25] P. H. Schönemann, "A generalized solution of the orthogonal Procrustes problem", *Psychometrika*, vol. 31, pp. 1–10, 1966.

[26] J. R. Hurley and R. B. Cattell, "The Procrustes program: Producing direct rotation to test a hypothesized factor structure", *Behav. Sci.*, vol. 7, pp. 258–262, 1962.

[27] G. H. Golub and C. F. van Loan, *Matrix Computations*, Johns Hopkins University Press, Baltimore, MD, 1983.

[28] K. S. Arun, T. S. Huang, and S. D. Blostein, "Least-squares fitting of two 3-D point sets", *IEEE Trans. Pattern Anal. Mach. Intell.*, vol. 9, pp. 698–700, 1987.

[29] S. Umeyama, "Least-squares estimation of transformation parameters between two point patterns", *IEEE Trans. Pattern Anal. Mach. Intell.*, vol. 13, pp. 376–380, 1991.

[30] O. D. Faugeras and M. Hebert, "The representation, recognition, and locating of 3-D objects", *Int. J. Robotics Res.*, vol. 5, pp. 27–52, 1986.

[31] M. Froimowitz and S. Matthysse, "Geometrical correspondence between phenazocine and the enkephalins", *J. Med. Chem.*, vol. 29, pp. 573–578, 1986.

[32] B. K. P. Horn, "Closed-form solution of absolute orientation using unit quaternions", *J. Opt. Soc. Amer. A*, vol. 4, pp. 629–642, 1987.

[33] David G. Kendall, "A survey of the statistical theory of shape", *Statistical Science*, vol. 4, pp. 87–120, 1989.

[34] C. Goodall, "Procrustes methods in the statistical analysis of shape", *J. R. Statist. Soc. B*, vol. 53, pp. 285–339, 1991.

[35] Fred L. Bookstein, *Morphometric tools for landmark data*, Cambridge University Press, Cambridge, 1991.

[36] S. K. Ghosh, *Analytical Photogrammetry*, Pergamon Press, New York, 2nd edition, 1988.

[37] B. K. P. Horn, *Robot Vision*, MIT Press, Cambridge, MA, 1986.

[38] P. H. Schönemann and R. M. Carroll, "Fitting one matrix to another under choice of a central dilation and a rigid motion", *Psychometrika*, vol. 35, pp. 245–255, 1970.

[39] B. F. Green, "The orthogonal approximation of an oblique structure in factor analysis", *Psychometrika*, vol. 17, pp. 429–440, 1952.

[40] A. C. Evans, S. Marrett, D. L. Collins, and T. M. Peters, "Anatomical-functional correlative analysis of the human brain using three dimensional imaging systems", *Medical Imaging III: Image Processing*, vol. Proc. SPIE 1092, pp. 264–274, 1989.

[41] C. R. Maurer, Jr., J. J. McCrory, and J. M. Fitzpatrick, "Estimation of accuracy in localizing externally attached markers in multimodal volume head images", *Medical Imaging 1993: Image Processing*, vol. Proc. SPIE 1898, pp. 43–54, 1993.

[42] S. C. Strother, J. R. Anderson, X.-L. Xu, J.-S. Liow, D. C. Bonar, and D. A. Rottenberg, "Quantitative comparisons of image registration techniques based on high-resolution MRI of the brain", *J. Comput. Assist. Tomogr.*, vol. 18, pp. 954–962, 1994.

[43] P. F. Hemler, S. Napel, T. S. Sumanaweera, R. Pichumani, P. A. van den Elsen, D. Martin, J. Drace, and J. R. Adler, "Registration error quantification of a surface-based multimodality image fusion system", *Med. Phys.*, vol. 22, pp. 1049–1056, 1995.

[44] K. Darabi, P. Grunert, and A. Perneczky, "Analysing the relationship between fiducial position and the geometrical error of intraoperative navigation", *Comput. Aided Surg.*, vol. 2, pp. 224, 1997 (Abstract from the conference *Computer Integrated Surgery 1997*).